Global Change Biology (2016), doi: 10.1111/gcb.13368

Crop connectivity under climate change: future environmental and geographic risks of potato late blight in Scotland

PETER SKELSEY, DAVID E. L. COOKE, JAMES S. LYNOTT and ALISON K. LEES
The James Hutton Institute, Invergowrie, Dundee DD2 5DA, UK

Abstract

The impact of climate change on dispersal processes is largely ignored in risk assessments for crop diseases, as inoculum is generally assumed to be ubiquitous and nonlimiting. We suggest that consideration of the impact of climate change on the connectivity of crops for inoculum transmission may provide additional explanatory and predictive power in disease risk assessments, leading to improved recommendations for agricultural adaptation to climate change. In this study, a crop-growth model was combined with aerobiological models and a newly developed infection risk model to provide a framework for quantifying the impact of future climates on the risk of disease occurrence and spread. The integrated model uses standard meteorological variables and can be easily adapted to various crop pathosystems characterized by airborne inoculum. In a case study, the framework was used with data defining the spatial distribution of potato crops in Scotland and spatially coherent, probabilistic climate change data to project the future connectivity of crop distributions for *Phytophthora infestans* (causal agent of potato late blight) inoculum and the subsequent risk of infection. Projections and control recommendations are provided for multiple combinations of potato cultivar and CO_2 emissions scenario, and temporal and spatial averaging schemes. Overall, we found that relative to current climatic conditions, the risk of late blight will increase in Scotland during the first half of the potato growing season and decrease during the second half. To guide adaptation strategies, we also investigated the potential impact of climate change-driven shifts in the cropping season. Advancing the start of the potato growing season by 1 month proved to be an effective strategy from both an agronomic and late blight management perspective.

Keywords: climate change, connectivity, crop disease, dispersal, inoculum, *Phytophthora infestans*, potato late blight, risk assessment

Received 29 January 2016 and accepted 18 April 2016

Introduction

The aerial dispersal of pathogen inoculum to uninfected hosts is crucial to the epidemic phase of many crop diseases (van Keulen & Stol, 1995; Skelsey, 2008; Skelsey *et al*., 2009a; Skelsey & Newton, 2014). Nevertheless, inoculum influx is largely ignored in climate change risk assessments for crop diseases, in part due to the mathematical complexity of dispersal models, but especially due to prediction uncertainties stemming from the stochastic nature of dispersal processes, as a result of the idiosyncrasies of the weather and the difficulty of knowing the locations of inoculum sources (Spitters *et al*., 1989). Instead, it is generally assumed that inoculum is ubiquitous, that is that the influx of inoculum will always occur at significant levels, so that future risk of disease is dependent only on local conditions for infection. So although risk models have been used to make spatial projections under future climates, for example disease risk maps, they are usually developed and applied exclusively in environmental space and not geographic space. Consequently, climate change risk assessments for crop disease epidemics may misrepresent future growing seasons (Skelsey & Newton, 2014).

Increasing recognition of the impact of global warming on the intensity and pattern of near-surface winds through, in particular, large-scale circulation changes, further undermines the assumption of ubiquitous inoculum at significant levels in climate change risk assessments for crop diseases (Pryor & Barthelmie, 2010; Hueging *et al*., 2013; Fant *et al*., 2015; Tobin *et al*., 2015; Johnson & Erhardt, 2016). For example, a recent modelling study found significant effects of projected wind speeds on the dispersal capacity of several British plant species under different CO_2 emissions scenarios (Bullock *et al*., 2012). Other determinants of inoculum dispersal, such as increased atmospheric turbulence, might also be altered as the climate warms. Kuparinen

Correspondence: Peter Skelsey, tel. +44 (0)1382 568 913,
fax +44 (0)844 928 5429, e-mail: peter.skelsey@hutton.ac.uk

et al. (2009) demonstrated that warmer conditions in a boreal forest led to greater turbulence in the airflow and, using this finding in a mechanistic wind dispersal model, predicted that dispersal distances could increase under climate warming. Climate change will also affect crop growth and phenology (e.g., Rötter & van de Geijn, 1999; Porter & Semenov, 2005; Kang *et al.*, 2009; Lobell & Gourdji, 2012), which impacts field-to-field inoculum dispersal through the effects of canopy height and structure on the escape, transportation, and deposition of inoculum (Aylor, 1990). Historically, growers have responded to climatic effects on crop growth by altering the dates of cropping seasons to maximize yield (Barnett *et al.*, 2006; Liu *et al.*, 2010), and this in turn can affect the coincidence of inoculum production, suitable weather for inoculum transportation, and the presence of host plants at a susceptible growth stage (Skelsey & Newton, 2014). These studies suggest that climate change could affect field-to-field inoculum dispersal both directly through changes to wind and turbulence, and indirectly through changes to crop growth and phenology and the ensuing effect on agronomic practices. A priority is to develop a methodology for projecting the unfolding consequences of climate change that can account for the limiting effect of inoculum abundance on infection risk.

In this study, we develop a modelling framework for quantifying the risk posed by aerially dispersed crop pathogens under climate change. Specifically, we model the interaction of climate, crop growth, dispersion of inoculum among crop locations and infection under a range of future climate scenarios. Our goals were to: (i) present a modelling framework that uses standard meteorological variables to provide a quantitative assessment of the connectivity of agricultural landscapes for inoculum and the subsequent risk of infection; and (ii) demonstrate the utility of the framework in a case study of the potential climate change effects on dispersal and disease risk for *Phytophthora infestans* (causal agent of potato late blight) inoculum in Scotland. The choice of the late blight pathosystem as a case study is pertinent due to the importance of potato to the global economy, the strong influence of weather conditions on epidemic spread at the landscape scale (Skelsey *et al.*, 2010), and the availability of validated models of the late blight pathosystem. Scotland was selected as the study area due to the availability of data on the spatial coverage of potato crops and the importance of late blight as a constraint to potato production. To guide adaptation strategies, we also considered agronomic scenarios regarding potential climate change-driven shifts in the dates of cropping seasons, as this could affect the coincidence of inoculum and suitable weather for disease development.

Materials and methods

General approach

We utilized an existing model of crop connectivity for *P. infestans* inoculum and developed a complementary model for risk of infection from deposited sporangia. The model of crop connectivity quantifies the potential of each crop location to produce inoculum and the further dispersion of inoculum to additional locations. It is comprised of a parsimonious 'temperature sum' crop growth model, and a model of the aerial component of the potato late blight disease cycle, both of which are components of a whole-pathosystem, spatiotemporal late blight simulator that has been empirically parameterized and validated (Skelsey *et al.*, 2005, 2007, 2009a,b,c, 2010, 2013; Skelsey, 2008; Zhang *et al.*, 2014). The modelled interaction of the crop-growth and spore-dispersion components is illustrated in Fig. 1. Projections for crop connectivity were driven using monthly 25 km gridded spatially coherent, probabilistic climate projections. The infection risk model was developed using data from controlled environment experiments with contemporary *P. infestans* genotypes and representative potato cultivars. Projections of infection risk under future climates were driven using synthetic weather sequences produced by a weather generator. Both the crop connectivity and infection risk models were implemented using data on the spatial coverage of potato crops in Scotland to account for realistic distributions of inoculum sources and recipients.

Crop distribution data

Approximately 95% of the total arable cropping area of Scotland is limited to the eastern seaboard of the country; a relatively small, flat area of nutrient-rich soil comprised of a near-continuous coastal strip from the English border to the Cromarty Firth. Results from recent studies suggest that climate change in Scotland over the next century would need to be greater than currently projected to be a major factor in the modification of agricultural planting patterns (Kerr *et al.*, 1999; Hay *et al.*, 2000; DEFRA 2012). We therefore assumed that the current spatial coverage of seed and ware potato crops in Scotland provided a reasonable proxy indicator for future distributions of *P. infestans* inoculum sources. Annual data defining the spatial coverage of seed potato crops were derived from the 'Seed Potato Unified Data System (SPUDS)': a database of bi-annual seed crop inspection records maintained by Science and Advice for Scottish Agriculture (SASA), a division of the Scottish Government Agriculture, Food and Rural Communities Directorate. Annual data defining the spatial coverage of ware potato crops in Scotland were derived from the Scottish Integrated Administration and Control System (IACS) (http://rpa.defra.gov.uk) and June Scottish Agricultural Census (http://www.scotland.gov.uk). These data are protected and are only available to the public in a high level summary form using the links provided. To capture variation in the distribution of potato crops between years, data from six different growing seasons (2006–2011) were used.

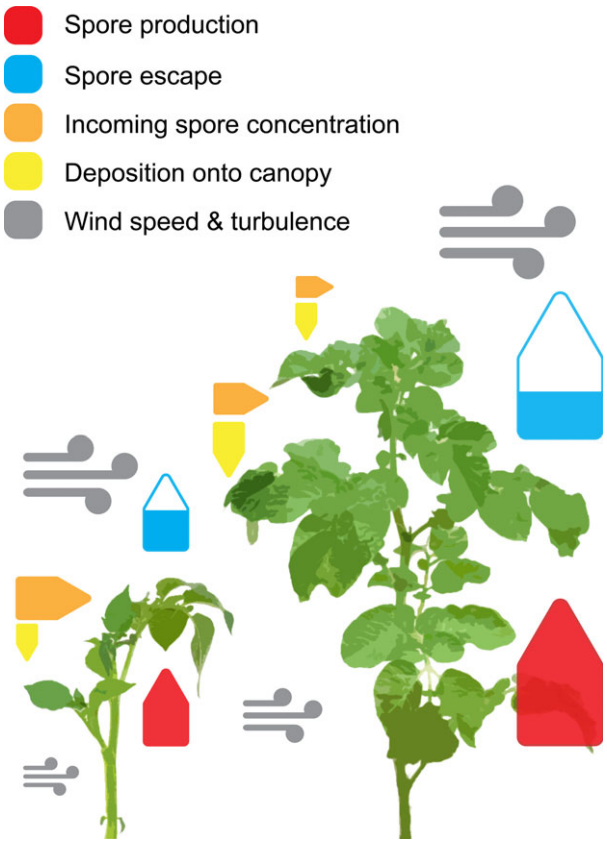

Fig. 1 Modelled interaction of host growth and inoculum transmission among crops. Spore production is proportional to canopy area, as large or full canopies have more healthy tissue available for colonization than growing or senescing crops. Conversely, the fraction of spores that escape up through the canopy and into the air above to become available for transportation by wind and turbulence is inversely proportional to canopy area; large or full canopies are more dense than growing or senescing crops therefore inoculum is more likely to deposit within the source crop. Crop height serves to counter this effect as wind speeds increase with height both within and above the canopy, meaning that spores in taller (not denser) crops will be more efficiently removed from infected plants. Similarly, the fraction of spores that escape the canopy to become available for long-distance transportation will encounter higher wind speeds with increased turbulence in the air above the canopy. Crop height also affects the interception of airborne inoculum by the upper canopy layers, as the vertical concentration profile of spores in a dispersing plume typically decreases with height due to the settling of spores down towards the surface due to gravity. Deposition onto host tissue is greater in large or full canopies due to the filtering effect of a larger surface area of leaves compared to the ground area of the crop.

Each individual crop distribution provided a different proxy of future coverage; that is, we considered these data as six different realizations of future crop coverage. These vector data sets were rasterized to 30 arcs grids. This resolution provided sufficient spatial detail to capture the configuration of crop distributions and was computationally tractable.

Weather data for climate change scenarios

Raw monthly 25 km gridded climate data (mean temperature, cloudiness and wind speed) from the UK Met Office Climate Projections database (UKCP09) 11-member ensemble of spatially coherent climate projections (SCPs) were used to drive the crop connectivity model. The SCPs provide the best estimates for modelling and summarizing the potential effects of future climates on epidemic spread in the United Kingdom as they are fully coherent across different locations, allowing the user to consider climate change at more than one location in a way that captures the relationship between the different locations, and to average projections across user defined land areas. They include both internal modelling variability (using perturbed physics ensembles) and external modelling variability (from the use of different General Circulation Models, or GCMs), as well as information on climate variability. The SCPs provide 11 equally plausible snapshots of climate change for a number of different emissions scenarios and time periods, and are freely available for download at http://ukclimateprojections.defra.gov.uk/. Two thirty-year future time slices (2030–2059, 2070–2099) and two climate forcing scenarios (UKCP09 Low and High) were used. UKCP09 1961–1991 baseline data were used for comparison, making a total of five climate change scenarios: baseline, Lo 2040s, Hi 2040s, Lo 2080s, Hi 2080s. Monthly data values from May to October were used, in order to fully encompass the potato growing season in Scotland; from the planting of 'first early' potato cultivars to the harvesting of 'late main' crops. These data were resampled from their original cell size to match the spatial resolution of the crop distribution data using nearest neighbour assignment so as to preserve the original values assigned within each 25 km grid cell.

The infection risk model was driven using hourly 5 km gridded time series of temperature and relative humidity. These were produced using the UK Met Office Climate Projections Weather Generator (UKCP09WG; http://ukclimateprojections.metoffice.gov.uk/). The UKCP09WG, by default, produces 100 simulations of 30 years of hourly time series for the baseline period (1961–1995) and a minimum of 100 time series for a future 30-year time period. The full 3000-sequence output from UKCP09WG for each emission scenario and crop location (over 36 000) resulted in unworkable computer expense; therefore, time series were generated for a sample of 15 crop locations. Five crop locations were selected from each of the three different climate regions of Scotland (as defined by the UK Met Office; http://www.metoffice.gov.uk/climate/uk/regional-climates): Northern, Eastern and Western Scotland. In general, the east and south tend to be drier, warmer, sunnier and less windy than the west and north. The number of data sequences carried through to modelling was further reduced to 100 synthetic years per scenario and location using Latin Hypercube sampling (McKay *et al*., 1979): see Darch *et al*. (2011) and von Christierson *et al*. (2012) for example methodologies. Monthly averages for temperature and number of hours per day

of relative humidity ≥90% were then determined from the yearly sequences to obtain climate data matching the temporal resolution of the UKCP09 SCPs.

Spatially explicit, weather-based model of crop connectivity for inoculum

Crop-growth submodel. We used the crop-growth model from a previously published potato late blight simulator as described in full by Skelsey *et al*. (2009c); therefore, only a summary is given here. It uses a thermal time approach and can be easily parameterized for different crop species. The model operates with a daily time step; therefore, a spline interpolation technique was used to downscale monthly projected temperature data to a daily temporal resolution. This simple downscaling technique was preferred to the use of daily UKCP09WG data because the spatial coherence of the downscaled climatic fields is preserved, and coherence is required for consideration of climate information simultaneously at multiple crop locations. Leaf area development was simulated through thermal time accumulation by computing the degree days during plant growth as the positive difference between the (average daily) temperature and a base temperature (2 °C) below which leaf growth stops. Leaf area index (*LAI*; m^2 leaf per m^2 ground) was initialized at 0.05 and increase in *LAI* modelled as a logistic function of growing degree days. *LAI* increased until the temperature sum reaches a maximum value, at which point net leaf growth became net leaf death. Shedding of leaves (senescence) was also calculated as a logistic function of growing degree days. The height of the crop was modelled as being proportional to *LAI*, as was the percentage of ground cover. We modelled two different notional cultivars of potato: an early maturing cultivar and a late maturing cultivar. Maturity class determined the growth duration of the crop and hence the period of time during which meteorology could affect inoculum dispersal. To investigate the interaction between climate change, maturity class and crop connectivity for *P. infestans* inoculum, we first simulated an early maturing potato cultivar at all crop locations, and then in a separate set of projections we simulated a late maturing variety, thus producing two sets of independent results. For early maturing cultivars, the growing season (emergence to harvest) lasted from May to August (inclusive), whilst for late varieties the growing season lasted from May to October (inclusive). Senescence began at 500 degree days for an early variety and 1000 degree days for a late variety. Maturity class also determined the height and density of the canopy and hence the influence of canopy structure on meteorology and crop connectivity. Early and late maturing cultivars grew and senesced at the same relative rates and required the same amount of time to reach a fully developed canopy; however, the maximum attainable *LAI* was three for an early variety and five for a late variety. The model was implemented at a 30 arcs resolution; that is, individual plants or crops were not simulated and host growth within individual grid cells containing potato was assumed to be homogeneous. To elucidate the effects of maturity class on the connectivity of crop distributions for inoculum transportation, crop distributions were assumed to be homogeneous for each maturity class in turn; that is, we did not associate maturity class with specific locations (grid cells) and performed two sets of projections (either early or late maturing crop distributions) for each emissions scenario.

Spore-dispersion submodel. The spore-dispersion submodel has three components: a term for spore production capacity, a mechanistic model for spore escape through the canopy, and an atmospheric dispersion model for transportation of escaped spores by wind and turbulence and deposition on distant potato crops. The spore escape model was originally developed and validated for the escape of *Sclerotinia sclerotiorum* ascospores from a grass canopy (de Jong *et al*., 2002). The atmospheric dispersion model is an internationally recognized partial reflection Gaussian plume model (Overcamp, 1976). The integrated spore-dispersion model used here has previously been validated and used for the dispersion of *P. infestans* sporangia (Skelsey, 2008; Skelsey *et al*., 2010), *Leptosphaeria maculans* ascospores (Zhang *et al*., 2014) and *Gibberella zeae* ascospores (Skelsey & Newton, 2014). It can be easily parameterized for different crop pathogens provided the terminal velocity of propagules is known (the speed at which they fall in the atmosphere). As the model has previously been fully described in these citations, we provide only the salient points required to repeat our analyses. The model was implemented at a monthly and 30 arcs resolution, using projected values for cloudiness and wind speed, together with the final computed values in each calendar month for crop height, *LAI*, and percentage ground cover from the crop-growth submodel (Fig. 1). Each grid cell containing potato was assumed to be a potential source of inoculum. In the absence of a quantitative model to predict the influence of weather on survival of overwintering sources of *P. infestans* inoculum and subsequent spore production in Scotland, we made the simplifying assumption that spore production at each source is computed by the product: *area of host tissue* (*LAI* × crop ground area) × *sporulating proportion of the canopy* (fixed at 0.01) × *sporulation intensity* (set to 1×10^8 spores m^{-2}). The proportion of inoculum in each crop that could escape up through the canopy and into the air above the canopy surface was calculated using the mechanistic model for spore escape, as a function of *LAI*, the terminal velocity of *P. infestans* sporangia, and wind speed within the crop. A power law profile for wind speed was used to correct projected wind speeds (10 m height) for heights within the canopy; this is a reasonable assumption in the absence of sufficient weather variables to parameterize boundary layer meteorology. The wind shear exponent of the power law profile was set to 1/7 for relatively flat terrain (Arya, 1999).

Transportation of escaped spores by wind and turbulence from each potato crop to all other potato crops was computed using the partial reflection Gaussian plume model. Lateral and vertical plume spread in the model depended on atmospheric stability (amount of turbulence or mixing in the air), which was parameterized using projected values of wind speed and cloudiness, together with season (month) and time of day (day or night), according to a scheme developed by the

Royal Dutch Meteorological Institute (KNMI). Briggs interpolation formulae were then used to compute the horizontal and vertical standard deviation of the plume concentration distribution as a function of atmospheric stability and downwind distance (Briggs, 1973). Potato crop locations were considered to be directly downwind from each inoculum source at some point during each monthly time step, thereby eliminating the need for wind direction in the model. The Gaussian plume model was used to predict the cumulative concentration (no. m^{-3}) of sporangia (emanating from all inoculum sources) arriving at each potato grid cell. The most important physical characteristic of a *P. infestans* sporangium, as regards deposition onto the leaf canopy, is its measured terminal velocity (0.0085 m s^{-1}), and this was used together with *LAI* to calculate the deposition flux (no. m^{-2}) onto host tissue at crop height. Note that all vertical coordinates in the dispersion model were adjusted by the 'displacement height', which accounts for the fact that in the presence of a crop canopy the surface over which the wind blows is not at the ground level but displaced by a height that is a function of the crop height. Deposition flux was then multiplied by the area of potato and the percentage ground cover in each grid cell to obtain a surface of the cumulative number of spores emanating from all potato crop locations that deposited on host tissue. As we did not simulate temporal epidemic dynamics, the monthly spore deposition distributions are interpreted as independent 'snapshots' of the environmental and geographic risks of inoculum transmission at various stages throughout a growing season, as opposed to a temporal series that embodies the build-up of inoculum during an epidemic event. More specifically, the spore deposition distributions quantify the connectivity of agricultural landscapes for airborne inoculum as a function of climate, the abundance, spatial arrangement and growth stage of inoculum sources and host crops, and the ability of the pathogen to move among them.

Weather-based model of infection risk

The infection efficiency of *P. infestans* propagules is assumed to peak at an optimum temperature and decreases towards zero as temperatures rise above or fall below this optimum. In contrast, the response of infection efficiency to leaf wetness duration (*LWD*) increases until the *LWD* value reaches an upper limit and is negligible if wetness duration is too short. Many foliar diseases exhibit this pattern of interaction between temperature, moisture and infection (Duthie, 1997; Monroe *et al*., 1997; Dalla Pria *et al*., 2006; Soares *et al*., 2008; Christiano *et al*., 2009; Gamliel-Atinsky *et al*., 2009; Launay *et al*., 2014). To describe the effects of both daily temperature and *LWD* on risk of infection, a surface response function was developed and fitted using data from controlled environment experiments and two of the most commonly found *P. infestans* lineages in the United Kingdom and Europe. Although this model is specific to *P. infestans*, our experimental approach can be replicated for similar foliar diseases. Alternatively, the temperature- and humidity-dependent parameters can be easily adjusted to suit the expected response as the main advantage of our approach is that the generic model can be used with subjective estimates of pathogen cardinal temperatures and wetness requirements for infection.

Experimental design. Seed of potato cultivar Maris Piper was planted in pots, and plants were grown for 4 weeks in a cool glasshouse in a randomized complete block design with four replicates. Plants were well spaced to produce sturdy plants that most closely reflect field behaviour and were inoculated just prior to flowering, the stage of growth at which resistance is best expressed (Stewart *et al*., 1983). No pesticides were applied.

Two isolates of *P. infestans*, 2009_7654A and 2009_7454A, obtained from naturally occurring late blight lesions in the United Kingdom and belonging to the highly aggressive and commonly found lineages 13_A2 and 6_A1, respectively (Cooke *et al*., 2012), were used in experiments. Cultures were established on Rye A agar in 9 cm Petri dishes, transferred onto leaves of the potato cultivar Craig's Royal and multiplied for several generations of 7–10 days (Andrivon *et al*., 2011) before being used experimentally. Inoculum was then multiplied on leaves of cultivar Craig's Royal for 7 days at 15 °C and high (90–100%) relative humidity (RH) after which time sporangia were released from the surface of the leaves by irrigation with sterile distilled water at room temperature. Sporangial suspensions were examined microscopically and the sporangial concentration adjusted to 1.4×10^4 ml^{-1} using a haemocytometer. Sporangial suspensions were not cooled to induce zoospore release as it was considered that this would give artificial results for treatments conducted at higher temperatures, where direct sporangial germination would be expected to occur under natural conditions. It is likely that zoospore release did occur in the lower temperature treatments, again accurately reflecting the biology of the pathogen.

Experiments were conducted at 6 temperatures (nominally 6, 10, 14, 18, 22, 24 °C), in combination with incubation of plants at each of those temperatures for a set number of hours (0, 1, 2, 4, 6, 8, 10, 14, 18, 24 h) at >90% RH postinoculation, where 90% RH is a proxy for leaf wetness. Controlled environment rooms were set at each of the different temperatures and the temperature (and humidity) was monitored hourly for the duration of the experiment by placement of Thermocron iButton temperature and humidity logging devices in each experimental box. The actual mean temperatures of the rooms during the experiments were found to be 8.6, 9.9, 13.4, 18.8, 21.7 and 23.3 °C, and the humidity within the boxes was maintained at >90% in all cases.

Nine, 160 l (h 60 cm × l 72 cm × w 48 cm) plastic boxes (Wham Crystal) with lids were placed into rooms set at each of the experimental temperatures and left for 3 h to acclimatize. Boxes were lined with damp tissue paper, and a glass beaker of water was placed in the corner of each box to maintain humidity. Ten plants were placed into each box, and four replicate boxes per temperature were individually inoculated with each of the two isolates. The ninth box, containing 10 uninoculated control plants, served as a negative control in each temperature tested. Humidity treatments were

randomized between the plants within boxes, and boxes inoculated with each isolate were randomized within the four replicates.

Phytophthora infestans inoculum was prepared as described above to give a suspension of 1.4×10^4 sporangia ml^{-1}. Misting equipment was turned on in the room whilst the lid was removed from individual boxes to maintain high humidity. A hand sprayer was used to apply the inoculum, and the spray was allowed to fall evenly from above onto the 10 plants in each box, and the lid was then replaced. One plant from each box was then removed at each of the 10 experimental timepoints between 0 and 24 h incubation (0, 1, 2, 4, 6, 8, 10, 14, 18, 24 h) and placed immediately in a glasshouse at 15 °C. The severity of late blight (proportion of diseased foliage) on each test plant was then assessed 7 and 10 days postinoculation according to the illustrated key of Cruikshank *et al.* (1982). We took the average severity value for the two *P. infestans* isolates and used that as a proxy for late blight infection risk.

Surface response function. We followed the approach of Launay *et al.* (2014) and used a Weibull equation to model infection risk, I (−), as a surface response to both temperature and *LWD* (hours of >90% RH):

$$I = \begin{cases} 0, & T < 0 \\ f(T)\{1 - \exp[-(A \cdot LWD)^B]\}, & T \geq 0 \end{cases} \quad (1)$$

where T is the air temperature during the period of wetness, $f(T)$ is a temperature response function that defines the upper symptote, and A and B are parameters. The temperature response function is a linear plateau function with ascending and descending portions on both sides of the optimal plateau:

$$f(T) = \begin{cases} 0, & T \leq T_{\min} \text{ and } T \geq T_{\max} \\ Y_{\max}, & T_{\text{opt1}} \leq T \leq T_{\text{opt2}} \\ \frac{Y_{\max}}{T_{\text{opt1}} - T_{\min}}(T - T_{\min}), & T_{\min} < T < T_{\text{opt1}} \\ \frac{Y_{\max}}{T_{\text{opt2}} - T_{\max}}(T - T_{\max}), & T_{\text{opt2}} < T < T_{\max} \end{cases} \quad (2)$$

where $Y_{\max}$ is the maximum proportion of diseased tissue under optimal conditions, and $T_{\min}$, T_{opt1}, T_{opt2} and $T_{\max}$ are the minimum, first optimum, second optimum and maximum temperatures for infection, respectively. To simplify the model we set $T_{min} = 0$. The fitted parameters were $A = 0.12$, $B = 1.84$, $Y_{\max} = 0.99$, $T_{\text{opt1}} = 10.42$, $T_{\text{opt2}} = 20.22$ and $T_{\max} = 25.34$ (Fig. 2).

Projected crop connectivity for the 2040s and 2080s

Monthly spore deposition distributions were generated using the 11-member ensemble of UKCP09 SCPs for all five of the CO_2 emissions scenarios on each of the six rasterized crop distributions data sets (six different realizations of future crop coverage). Within each crop distribution, we investigated geographic variability in climate by separately averaging spore deposition values over all potato grid cells within the three different climate regions of Scotland (Northern, Eastern and Western Scotland). This gave a superensemble of 66 (11 SCPs × 6 crop distributions) spore deposition values for each combination of month, climatic region and CO_2 emissions scenario. This process was repeated to produce two independent sets of projections, assuming (i) an early maturing potato cultivar or (ii) a late maturing cultivar at all locations. To summarize these results and facilitate interpretation by the potato industry, projected monthly values were averaged over the first half of the season (the period of rapid canopy growth from emergence to maximum *LAI* during which early preventative measures against foliar blight are possible) and the second half of the season (the period of full canopy closure until the beginning of senescence when protection of tubers from infection is important). The two halves of the season were defined as May to June (inclusive) and July to August for the early cultivar, and May to July and August to October for the late cultivar. Climate change-induced shifts in the cropping season are investigated in the 'Future agronomic scenarios' section. Results for future climates were taken relative to those for baseline conditions and presented as percentage changes in inoculum deposition using boxplots (computed from the superensemble of 11 SCPs × 6 crop distributions) to quantify uncertainty due to internal climate variation and future crop coverage. This gave a total of 12 boxplots per CO_2 emissions scenario: 2 potato cultivars × 3 climatic regions × 2 seasonal averages. Note that projections for the two potato cultivars are

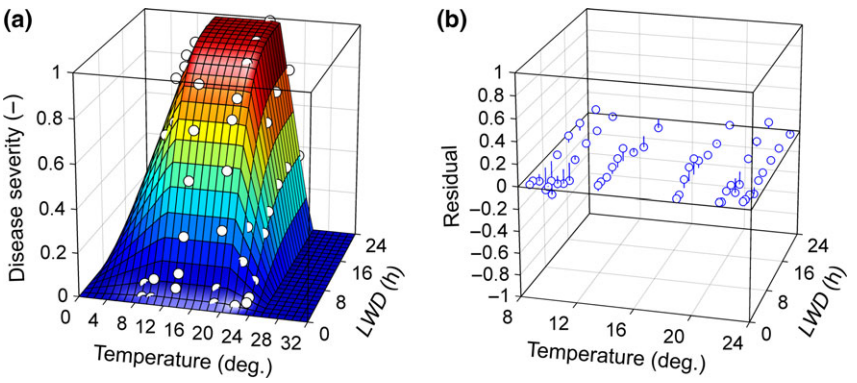

Fig. 2 Effects of leaf wetness duration, *LWD* (hours of >90% relative humidity) and temperature on the severity of potato late blight (proportion of diseased foliage) after one infection cycle, as predicted by (a) a surface response function, where data markers show observed values and (b) residuals of the model fit ($R^2 = 0.98$, standard error of residuals = 0.05).

qualitatively but not quantitatively comparable, due to the different growing seasons.

Projected risk of infection for the 2040s and 2080s

The infection risk model was developed using the two predominant *P. infestans* genotypes in Scotland and a susceptible potato cultivar and is therefore assumed to provide a conservative prediction of late blight risk for all areas of Scotland where potato is planted. Monthly values for risk of infection were generated using the UKCP09WG data for all five of the CO_2 emissions scenarios at each of the 15 sampled crop locations. Initial analyses revealed that differences in infection risk among the 15 crop locations were small, therefore the monthly projected values within each CO_2 emissions scenario were grouped into a superensemble (100 synthetic years × 15 locations). Although the infection risk model is independent of potato maturity class, the monthly projections were averaged over the first and second halves of the potato growing season for an early and a late maturing cultivar to provide projections that matched the seasonal averaging intervals of the crop connectivity projections. Results for future climates were taken relative to those for baseline conditions and presented as percentage changes in infection risk using boxplots (computed from the superensemble of 100 synthetic years × 15 locations), in order to quantify uncertainty due to internal climate variation and future crop coverage. This gave a total of four boxplots per CO_2 emissions scenario: 2 cropping periods, corresponding to the growing seasons for an early and a late maturing cultivar, × 2 seasonal averages.

Future agronomic scenarios – a climate change-induced shift in the cropping season

Climate change is likely to present opportunities for earlier growing seasons as warmer conditions arrive earlier in the year. To investigate the potential effect of planting crops 1 month earlier, we repeated all climate change risk projections using projected air temperatures for April–September ('adapted' growing season); as opposed to May–October for a 'standard' potato growing season in Scotland. Thus, an assumption was made that a comparable amount of primary inoculum would be available to initiate epidemics earlier in the growing season under a warmer climate. The two halves of the season were redefined as April to May (inclusive) and June to July for an early maturing cultivar, and April to June and July to September for a late maturing cultivar. Distributions of projected values for crop connectivity and infection risk were examined using boxplots as described above.

Projected net impact of climate change and cropping period on overall risk of disease

It is useful to determine the projected net impact of climate change on overall risk of disease and to compare values for a standard and an adapted growing season. Net impact (total change) was calculated as the product of the factor changes in crop connectivity and infection risk. This is explained as follows. Crop connectivity quantifies the number of spores that deposit on host tissue and infection risk determines the proportion of those that can cause lesions; therefore, the total change in epidemic risk is the product of the factor changes in these sequential epidemic processes (Skelsey *et al*., 2009b). We did not compute regional averages for crop connectivity as described above, but instead grouped projected values for all crop locations into superensembles to match the superensembles of crop locations for infection risk. Results were averaged over the first and second halves of the growing season (standard and adapted) for early and late maturing potato cultivars as described above, and the median values for each combination of CO_2 emissions scenario, potato maturity class and seasonal average were determined.

Results

Crop distribution data

There were a total of 28 242 seed crops and 8105 ware crops in the set of six potato distributions. The mean number of crop locations per year was 6058 (range 5204–7315), and the mean crop area was 4.1 ha (range 0.001–25 ha). Interyear variability in the spatial coverage of potato crops was constrained by the small percentage of available prime quality agricultural land in Scotland, the majority of which is located in the eastern seaboard of the country (Fig. 3). This means that potato production tends to cluster geographically and fields are not situated far from the previous year's potato crop.

Weather data for climate change scenarios

Although future weather varied depending on which of the many scenarios were used, Scotland is projected to experience increasing average temperatures throughout the potato growing season, decreasing wind speeds and an overall reduction in cloudiness and RH, although there will be an increase in average rainfall in spring and autumn and a decrease in average rainfall in summer. For example, under the high CO_2 2080s scenario, the range of projected changes over the course of the first half (May to July, inclusive, across the 11-member ensemble of SCPs) of the full potato growing season in northern, eastern and western crop locations (across the set of six crop distributions), respectively, were as follows: +1.7 to +7.4 °C, +2.5 to +7.7 °C and +2.1 to +7.4 °C for mean temperature; −14.4 to +12.1%, −17.0 to +5.5% and −17.2 to +6.4% for cloudiness; −0.9 to +0.5 m s^{-1}, −0.8 to +0.7 m s^{-1} and −0.8 to +0.4 m s^{-1} for wind speed; and −9.9 to +7.4%, −12.5 to +5.0% and −13.5 to +4.1% for RH. The range of projected changes

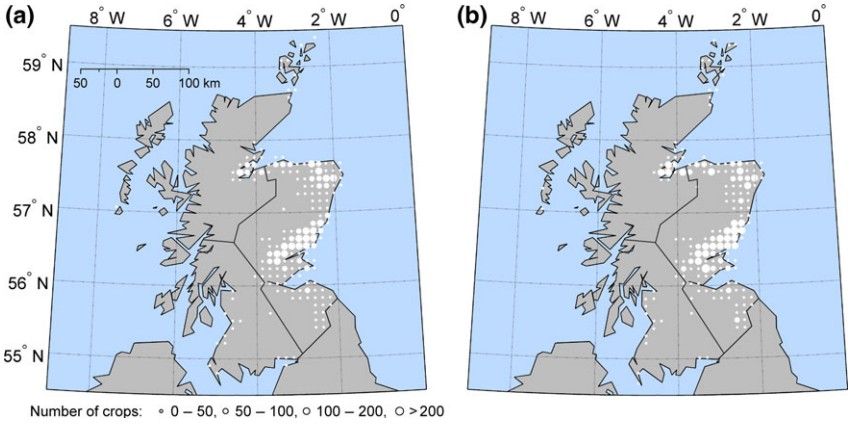

Fig. 3 Example map showing the distribution of potato (seed and ware) crops in (a) 2010 and (b) 2011. Internal boundaries show the demarcation of the UK Met Office Northern, Western and Eastern climate regions. Data have been aggregated to a 5 arcmin (approximately 10 × 10 km) grid for illustrative purposes and confidentiality reasons.

over the course of the second half (August to October, inclusive) of the full potato growing season in northern, eastern and western crop locations, respectively, were as follows: +2.1 to +7.8 °C, +3.1 to +8.3 °C and +2.7 to +8.2 °C for mean temperature; −19.1 to +22.7%, −22.1 to +9.5% and −22.7 to +6.2% for cloudiness; −1.4 to +0.9 m s^{-1}, −1.0 to +0.7 m s^{-1} and −1.1 to +0.7 m s^{-1} for wind speed; and −8.3 to +7.6%, −12.5 to +2.5% and −13.1 to +3.9% for RH. The projected climate trends were compatible with a review of recent historical climate trends in Scotland (Sniffer, 2014). Their analysis showed that Scotland has become warmer, wetter, less cloudy and less humid between 1961 and 2011: there has been a significant increase in average temperature for all seasons by between 1.0 to 1.6 °C; rainfall has increased significantly by 25% in the spring and 23% in the autumn, with little change in average summer rainfalls; sunshine duration has increased significantly by 0.6 h day^{-1} in spring and 0.3 h day^{-1} in autumn, with little change in summer; and there has been a significant decrease in average RH for all seasons by between 2.0% and 3.4%.

Projected crop connectivity for the 2040s and 2080s

Relative to baseline conditions, crop connectivity for *P. infestans* inoculum (i.e. cumulative spore deposition on host tissue at crop locations) was projected to increase during the first half of the growing season and decrease during the second half for both the early and late maturing potato cultivars under all future emissions scenarios (Fig. 4). The magnitudes of projected changes increased consistently with time and level of CO_2 emissions. There was notable geographic variability in the response of crop connectivity to climate change, with median change to current connectivity differing by as much as 11%, 13%, 5% and 13% among climatic regions during the first and second halves of the growing season for the early and late cultivar, respectively (Fig. 4a–d). The wide array of model and scenario outcomes suggests uncertainty in projections of future crop connectivity, although the trend for a within-season increase then decrease of connectivity over baseline conditions was clear. This was primarily because warmer temperatures (relative to baseline conditions) accelerated the growth of crops during the first half of the growing season, thereby increasing the amount of host tissue available for spore production, and accelerated the onset of senescence during the second half of the season, with a subsequent decrease in spore production capacity towards the end of the season. Nonetheless, change in *LAI* was insufficient to accurately quantify change in crop connectivity. A sensitivity analysis with the integrated model revealed that an increase in *LAI* (initially fixed at 1) of 5%, 25% and 50%, whilst keeping all other variables fixed at baseline values, produced an increase in the total number of spores deposited on host tissue of 12%, 89% and 217%, respectively (data not shown). A decrease in *LAI* (initially fixed at 5) of 5%, 25% and 50% produced a decrease in the total number of spores deposited on host tissue of 3.5%, 33% and 76%, respectively. The variations in sensitivity are due to nonlinear dependencies between crop- and dispersion-model components in the integrated model, such as the influence of canopy density on: spore production capacity, the fraction of spores that escape the canopy and become available for long-distance transport, and the proportion of dispersed spores that deposit on host tissue (Fig. 1). The importance of the spatial dimension of pathosystem epidemiology on model projections is

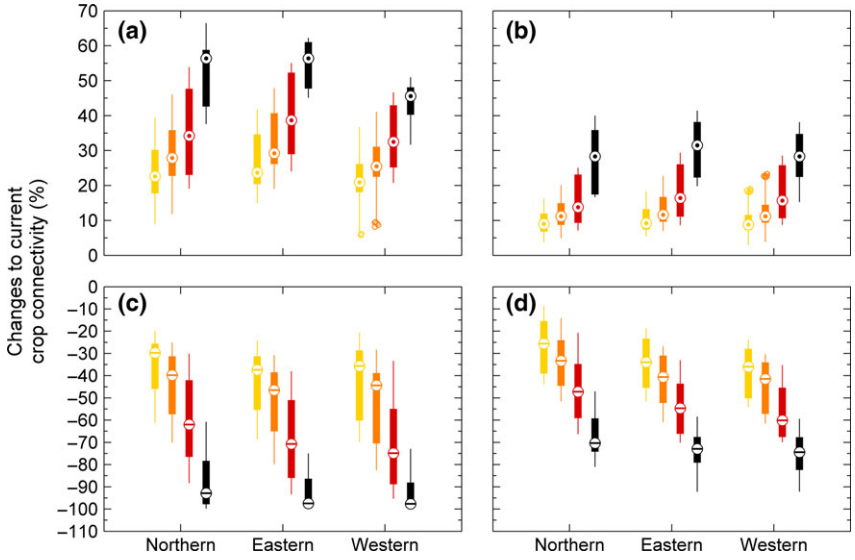

Fig. 4 Projected change in production, transportation and deposition of *Phytophthora infestans* inoculum on potato crops in Scotland. Boxplots show uncertainty due to internal climate variation and future crop coverage for spore deposition averaged over all potato crop locations in the Northern, Eastern and Western Scotland climate regions, and over two different seasonal intervals: the months comprising the first half of the potato growing season for (a, b) an early and late maturing potato cultivar, respectively, and the months comprising the second half of the growing season for (c, d) an early and late maturing potato cultivar, respectively. The two halves of the season were defined as May to June (inclusive) and July to August for the early cultivar, and May to July and August to October for the late cultivar. Colours of bars indicate the future CO_2 emissions scenario: yellow = low CO_2 2040s, orange = high CO_2 2040s, red = low CO_2 2080s and black = high CO_2 2080s. Projected values are expressed relative to the 1961–1991 baseline climatology to show the proportional response. Boxes extend from first to third quartile, medians are marked in each box (dots for the first half of the growing season and bars for the second half), and whiskers extend to the most extreme data points not considered outliers (circular markers).

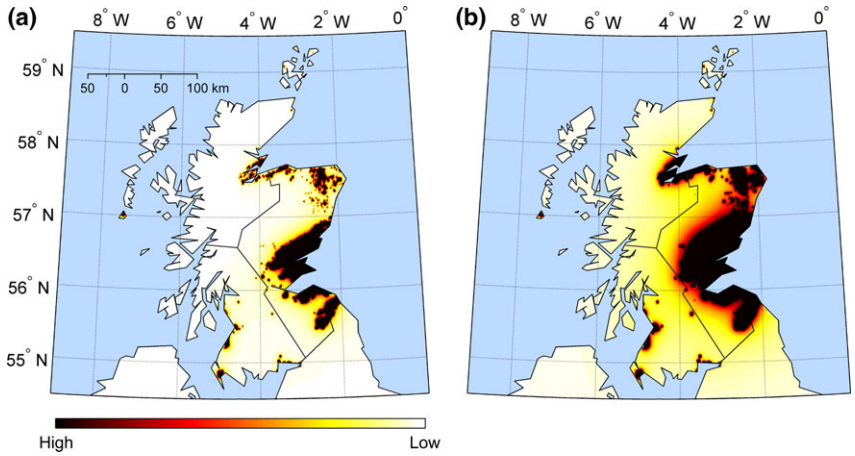

Fig. 5 Example maps showing the influence of future CO_2 emissions scenario on the spatial distribution of *Phytophthora infestans* inoculum. The two maps were produced using the same potato crop distribution as primary inoculum sources (Fig. 3b) and show spore deposition flux (no. m^{-2}) to all land cells during the first month (May) of the growing season for an early maturing potato cultivar under (a) baseline conditions and (b) a high CO_2 emissions scenario in the 2080s. Internal boundaries show the demarcation of the UK Met Office Northern, Western and Eastern climate regions.

further illustrated using maps of the spatial distribution of airborne inoculum, which reveal large differences in the movement of inoculum between crop locations under future climates (Fig. 5).

Projected risk of infection for the 2040s and 2080s

Relative to baseline conditions, the risk of infection increased when averaged over the months

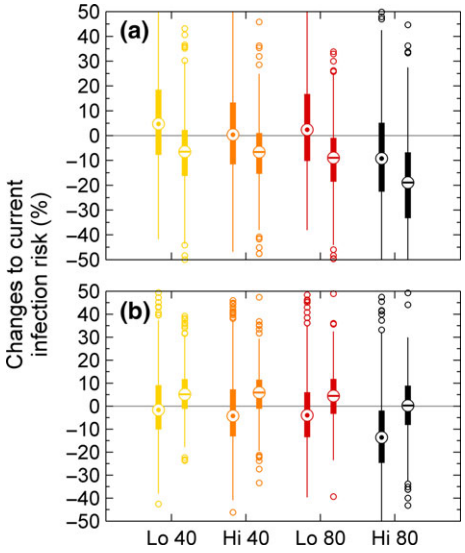

Fig. 6 Projected change in risk of infection by *Phytophthora infestans* inoculum in potato crop locations in Scotland. Boxplots show uncertainty due to internal climate variation and future crop coverage for risk of infection averaged over two different seasonal intervals: the months comprising the first (boxes with dots for medians) and second (boxes with bars for medians) halves of a growing season for (a) an early maturing potato cultivar, (b) and a late maturing potato cultivar. The two halves of the season were defined as May to June (inclusive) and July to August for the early cultivar, and May to July and August to October for the late cultivar. Colours of bars indicate the future CO_2 emissions scenario: yellow = low CO_2 2040s, orange = high CO_2 2040s, red = low CO_2 2080s and black = high CO_2 2080s. Projected values are expressed relative to the 1961–1991 baseline climatology to show the proportional response. Boxes extend from first to third quartile, medians are marked in each box, and whiskers extend to the most extreme data points not considered outliers (circular markers).

corresponding to the first half (May and June) of a growing season for early maturing cultivars, with the exception of the high CO_2 emissions scenario in the 2080s (Fig. 6a). Risk of infection decreased when averaged over the months comprising the second half (July and August) of a growing season for early maturing cultivars (Fig. 6a). These trends are consistent with the aforementioned projected and historical climate trends for Scotland. Warmer spring months (relative to current conditions) that favour infection produced an increase in risk during the first half of the growing season, with the exception of the high CO_2 2080s scenario where temperatures in June exceeded the optimum for infection (Fig. 2). Hotter, less humid summer months that inhibit infection produced a decrease in risk during the second half of the season.

Risk of infection decreased when averaged over the months corresponding to the first half (May to July, inclusive) of a growing season for late maturing cultivars and increased when averaged over the months comprising the second half (August to October, inclusive) of a growing season (Fig. 6b). These trends are again consistent with the aforementioned projected and historical climate trends for Scotland. Hotter, less humid summer months (relative to current conditions) that inhibit infection produced a decrease in risk during the first half of the growing season. Warmer autumn months produced an increase in risk during the second half of the growing season, with a magnitude of change that decreased as conditions exceeded the optimum for infection (Fig. 2).

Future agronomic scenarios – a climate change-induced shift in the cropping season

Crop connectivity decreased (relative to a standard growing season under baseline conditions) during the first half of the adapted cropping period for both early (April and May) and late (April to June, inclusive) maturing cultivars under all future CO_2 emissions scenarios, with the exception of the high CO_2 2080s scenario (Fig. 7a, b). This was primarily because advancing the start of the growing season by 1 month meant that the first half of the adapted growing season was cooler than that of a standard growing season under current conditions (with the exception of the high CO_2 2080s scenario), which slowed the growth of crops and reduced the amount of host tissue available for spore production. Crop connectivity for the early maturing cultivar increased during the second half (June and July) of the adapted cropping period under the 2040s emissions scenarios and decreased under the 2080s emissions scenarios (Fig. 7c). This was primarily because the second half of the adapted growing season (June and July) in the 2040s scenarios was cooler than that of a standard growing season (July and August) under current conditions, which slowed the onset of senescence and increased spore production potential towards the end of the season. Conversely, temperatures were warmer under the second half of an adapted growing season during the 2080s than a standard season under current conditions, which accelerated the onset of senescence and reduced spore production potential towards the end of the season. For the same reason, crop connectivity decreased during the second half of the adapted growing season for the late maturing cultivar under all emissions scenarios (Fig. 7d). Although advancing the start and end dates of the growing season shifted the first half of cropping periods towards windier spring months that favour spore transportation, and shifted the second half of cropping periods away from windier autumn months towards

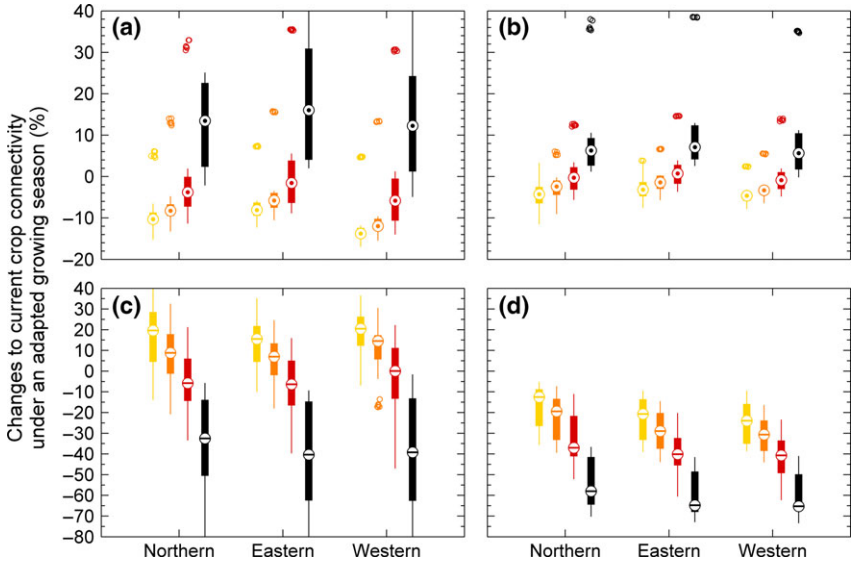

Fig. 7 Projected change in production, transportation, and deposition of *Phytophthora infestans* inoculum on potato crops in Scotland under an adapted (1 month earlier) growing season. Boxplots show uncertainty due to internal climate variation for spore deposition averaged over all potato crop locations in the Northern, Eastern and Western Scotland climate regions, and over two different seasonal intervals: the months comprising the first half of the potato growing season for (a, b) an early and late maturing potato cultivar, respectively, and the months comprising the second half of the growing season for (c, d) an early and late maturing potato cultivar, respectively. The two halves of the season were defined as April to May (inclusive) and June to July for the early cultivar, and April to June and July to September for the late cultivar. Colours of bars indicate the future CO_2 emissions scenario: yellow = low CO_2 2040s, orange = high CO_2 2040s, red = low CO_2 2080s and black = high CO_2 2080s. Projected values for the shifted growing season are expressed relative to the 1961–1991 baseline climatology under a standard growing season to show the proportional response. Boxes extend from first to third quartile, medians are marked in each box (dots for the first half of the growing season and bars for the second half), and whiskers extend to the most extreme data points not considered outliers (circular markers).

calmer summer months, the effects on crop connectivity were overwhelmed by the changes in spore production capacity (i.e. the amount of host tissue available for spore production). A comparison of projected values for adapted growing seasons (Fig. 7) with projected values for standard growing seasons (Fig. 4) showed that advancing the start and end dates of the growing season by 1 month served to decrease future crop connectivity during the first half of a growing season and increase future crop connectivity during the second half, under all future emissions scenarios.

Risk of infection increased (relative to a standard growing season under baseline conditions) when averaged over the months comprising the first half of an adapted growing season for both an early and a late maturing cultivar and decreased when averaged over the months comprising the second halves of their respective growing season (Fig. 8). This is because advancing the start and end dates of the growing season shifted the first half of cropping periods away from warmer, less humid summer months towards cooler, more humid spring months that favoured infection, and shifted the second half of cropping periods from cooler, more humid autumn months towards hotter, less humid summer months that inhibited infection. A comparison of projected values for adapted growing seasons (Fig. 8) with projected values for standard growing seasons (Fig. 6) shows that advancing the start and end dates of the growing season by 1 month increased infection risk during the first half of a growing season and decreased infection risk during the second half, under all future CO_2 emissions scenarios.

Projected net impact of climate change on overall risk of disease

Under a standard growing season, the overall risk of disease always increased (factor change >1) during the first half of the season and decreased (factor change <1) during the second half (Table 1). The same was true under an adapted growing season, with the exception of the early maturing cultivar during the second half of the season in the 2040s. The magnitudes of projected changes to current late blight risk were smaller under an adapted growing season in almost all combinations of potato maturity class, seasonal average and CO_2 emissions scenario.

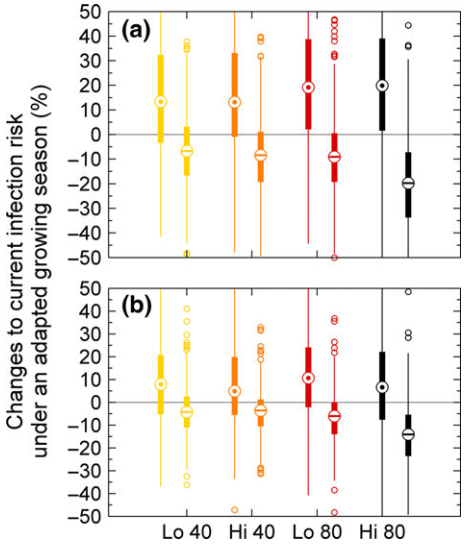

Fig. 8 Projected change in risk of infection by *Phytophthora infestans* inoculum in potato crop locations in Scotland under an adapted (1 month earlier) growing season. Boxplots show uncertainty due to internal climate variation and future crop coverage for risk of infection averaged over two different seasonal intervals: the months comprising the first (boxes with dots for medians) and second (boxes with bars for medians) halves of an adapted growing season for (a) an early maturing potato cultivar, (b) and a late maturing potato cultivar. The two halves of the season were defined as April to May (inclusive) and June to July for the early cultivar, and April to June and July to September for the late cultivar. Colours of bars indicate the future CO_2 emissions scenario: yellow = low CO_2 2040s, orange = high CO_2 2040s, red = low CO_2 2080s and black = high CO_2 2080s. Projected values for the shifted growing season are expressed relative to the 1961–1991 baseline climatology under a standard growing season to show the proportional response. Boxes extend from first to third quartile, medians are marked in each box (dots for the first half of the growing season and bars for the second half), and whiskers extend to the most extreme data points not considered outliers (circular markers).

Table 1 Projected net impact of climate change on risk of potato late blight in Scotland under a standard growing season and an adapted growing season. Net impact is calculated as the product of factor changes to current spore transportation among crops and current infection risk

Potato maturity* class/ half season interval	Low CO_2 2040s	High CO_2 2040s	Low CO_2 2080s	High CO_2 2080s
Factor change to current late blight risk under a standard growing season†				
Early/1st	1.25	1.27	1.35	1.37
Late/1st	1.07	1.06	1.11	1.12
Early/2nd	0.60	0.52	0.30	0.03
Late/2nd	0.69	0.64	0.47	0.27
Factor change to current late blight risk under an adapted growing season				
Early/1st	1.01	1.04	1.16	1.39
Late/1st	1.04	1.02	1.11	1.14
Early/2nd	1.11	1.00	0.87	0.51
Late/2nd	0.76	0.69	0.57	0.32

*The standard growing season ran from May through to August (inclusive) for an early maturing potato cultivar, and May through to October for a late maturing cultivar. The start and end dates of the adapted growing were advanced by 1 month. Projected values were averaged over the 1st and 2nd halves of the growing season.
†Median values computed from superensembles of model projections at all crop locations.

Discussion

In this study, we used a combination of mechanistic models for crop growth, spore escape, spore transportation and deposition, and infection to quantify the connectivity of agricultural landscapes for crop pathogens and the subsequent infection risk under future climates and cropping regimes. The explanatory power of the individual submodels allowed numerous conclusions to be drawn regarding the chosen case study of potato late blight in Scotland. The results for the first half of the growing season are especially significant, as early preventative measures are considered crucial in averting large-scale potato late blight epidemics (Stevenson, 1993; Cooke *et al.*, 2011; British Potato Council, 2013). A key finding for the potato industry is that crop connectivity is projected to increase during the first half of the growing season under all future CO_2 emissions scenarios (Fig. 4), and these increases far outweigh any change in the risk of infection (Fig. 6; Table 1). In the United Kingdom, the majority of potato growers follow a 'routine spray schedule' (according to the calendar) for the application of fungicides that prevent infection from depositing spores. Products are typically applied at 7–10-day intervals that can be further adjusted according to the prevailing risk, and the first spray is traditionally applied prior to canopy closure (British Potato Council, 2013). The large projected increase in crop connectivity early in the season suggests that fungicide spray regimes may need to start earlier in the future, with shorter intervals between applications. There is potential, however, to offset additional fungicide applications by lengthening spray intervals during the second half of the season, as the projected decreases in crop connectivity again outweigh any slight increase in infection risk. Typically, studies of climatic indicators for crop disease risk consider only infection and results are averaged over what is considered to be the entire

critical period (e.g. Launay *et al.*, 2014; Sparks *et al.*, 2014). In this study, the median changes to current infection risk averaged over the entire potato growing season (May to October, inclusive) were 2.5%, 1.1%, 0.5% and −6.7% for the high and low CO_2 emissions scenarios in the 2040s and 2080s, respectively (Fig. 6b). These changes are markedly different to the half seasonal averages for different potato maturity classes (Fig. 6) and could be considered negligible, particularly in the absence of any information on future crop connectivity. This highlights the utility and novelty of our approach in including additional components of the disease cycle and using shorter averaging intervals that are more meaningful to the agricultural sector.

A second key finding for the potato industry concerns the ramifications of a climate change-induced shift in the cropping season. Results from the crop-growth model suggest that climate change will cause earlier maturation and senescence of potato crops in Scotland. These projected trends in the crop life cycle and our adaptation scenario regarding a climate change-induced shift in the cropping season are compatible with historical records. A recent analysis of approximately 4000 monthly temperature data sets for the period 1951–2010 showed that growing seasons in the United Kingdom were starting earlier and have lengthened by 3.8 growing degree days per year (Spinoni *et al.*, 2015). This was confirmed in another study of historical climate trends in Scotland for the period 1961–2003, which showed that the growing season has increased by more than 5 weeks since 1961 in all three climatic regions due to an earlier start of the growing season rather than an extension (Sniffer, 2014). A review of recent historical climate trends in Scotland showed a 25% reduction in the number of days of frost (both air and ground frost) across Scotland between 1961 and 2004, and consequently, growing season start dates (defined as starting when the temperature on five consecutive days exceeds 5 °C) have moved forward by approximately 3 weeks (Barnett *et al.*, 2006). This trend is expected to continue as warmer conditions are expected for Scotland in the future. The results of this study suggest that an earlier start to the cropping period will increase the resilience of Scottish potato production systems to the expected changes in climate and late blight risk, as the magnitudes of projected changes to current late blight risk were smaller under an adapted vs. a standard growing season. Thus, adaptation of the growing season to suit a warmer climate presents certain advantages from both an agronomic and late blight management perspective.

A third key finding for the potato industry concerns the marked geographic variability in the response of crop connectivity for *P. infestans* inoculum to climate change. This suggests there may be utility in shifting potato production to areas where conditions are less conducive to spread of late blight. However, the rugged topography and poor soil quality which applies in much of Scotland, tied to remoteness from main markets, makes viable and profitable arable crop farming a challenging task outside of the main potato production areas in the Eastern climatic region (Kerr *et al.*, 1999; Hay *et al.*, 2000; DEFRA, 2012). Of the three geographic regions, projected values of cumulative spore deposition were always lower in the Western climatic region. This was mainly due to the smaller number of crop locations acting as sources and receptors of inoculum. These projections were made using data on the existing spatial coverage of potato crops in the Western climatic region. Expansion of these existing operations in the Western climatic region could therefore be a risk-averse strategy to increase potato production by changing agricultural planting patterns.

A number of methodological limitations necessitate caution in interpreting the findings of this study. Most General Circulation Models (climate models) make projections at a relatively coarse resolution and cannot represent the fine scale detail that characterizes the climate in many regions of the world. UKCP09 probabilistic projections are designed to sample much of the uncertainty introduced by deficiencies in climate models by the use of perturbed physics and multimodel ensembles, but given the highly complex orography, heterogeneous land surface cover and coastlines of Scotland, some uncertainty remains as to the accuracy of projected climate variables. There are also uncertainties associated with the crop-dispersion model. Crop phenology was driven by the sum of daily air temperatures and did not include, for example precipitation and water exchange processes, nor the impact of atmospheric CO_2 concentration on crop growth. Similarly, more comprehensive and robust dispersion models are available; multiple validation studies have concluded that Gaussian plume models can predict atmospheric concentrations within a factor of two at distances of up to 20 km, but predictions over larger scales tend to be less accurate (de Visscher, 2013). However, the increased data requirements and computation time of more complex crop-growth and dispersion models preclude their use in this study due to the large number of crop locations considered (over 36 000) in each projection. In addition, our primary aim was to present a parsimonious projection framework comprised of biologically plausible models that use standard meteorological variables.

Our synthesis of a crop-growth model with models for the aerobiological pathway of crop pathogens and subsequent infection risk provides an integrated view

on the effects of climate change on the risk of crop disease occurrence and spread. This work demonstrates the importance of spatial context in climate change risk assessments for crop diseases, and consideration of the temporal and spatial coincidence of crop and pathogen species with conducive conditions for infection/growth/spread. We were able to demonstrate the utility of our approach in providing useful information to guide government and industry strategies for agricultural adaptation to climate change. The methodology developed in this study is extendable to other pathosystems characterized by airborne inoculum and can be applied using standard GCM output.

Acknowledgements

We are grateful for financial support for this work in part from the Rural and Environment Science and Analytical Services (RESAS) Division of the Scottish Government under its Environmental Change and Food, Land and People Strategic Research Programmes (2011–2016).

References

Andrivon D, Avendaño-Córcoles J, Cameron AM *et al*. (2011) Stability and variability of virulence of *Phytophthora infestans* assessed in a ring test across European laboratories. *Plant Pathology*, **60**, 556–565.

Arya SP (1999) *Air Pollution Meteorology and Dispersion*. Oxford University Press, New York.

Aylor DE (1990) The role of intermittent wind in the dispersal of fungal pathogens. *Annual Review of Phytopathology*, **28**, 73–92.

Barnett C, Hossell J, Perry M, Procter C, Hughes G (2006) *Patterns of climate change across Scotland: technical report*. SNIFFER Project CC03, Scotland & Northern Ireland Forum for Environmental Research.

Briggs GA (1973) *Diffusion estimates for small emissions (draft)*. Atmospheric Turbulence and Diffusion Laboratory, Contribution No. 70 (Draft), Oak Ridge, TN.

British Potato Council (2013) *Managing the Risk of Late Blight*. Agriculture and Horticulture Development Board, Stoneleigh Park, Warwickshire.

Bullock JM, White SM, Prudhomme C, Tansey C, Perea R, Hooftman DAP (2012) Modelling spread of British wind-dispersed plants under future wind speeds in a changing climate. *Journal of Ecology*, **100**, 104–115.

Christiano RSC, Dalla Pria M, Jesus Junior WC, Amorim L, Bergamin Filho A (2009) Modelling the progress of Asiatic citrus canker on Tahiti lime in relation to temperature and leaf wetness. *European Journal of Plant Pathology*, **124**, 1–7.

von Christierson B, Vidal JP, Wade SD (2012) Using UKCP09 probabilistic climate information for UK water resource planning. *Journal of Hydrology*, **424**, 48–67.

Cooke LR, Schepers HTAM, Hermansen A *et al*. (2011) Epidemiology and integrated control of potato late blight in Europe. *Potato Research*, **54**, 183–222.

Cooke DEL, Cano LM, Raffaele S *et al*. (2012) Genome analyses of an aggressive and invasive lineage of the Irish potato famine pathogen. *PLoS Pathogens*, **8**, e1002940.

Cruikshank G, Stewart HE, Wastie RL (1982) An illustrated assessment key for foliage blight of potatoes. *Potato Research*, **25**, 213–214.

Dalla Pria M, Christiano RCS, Furtado EL, Amorim L, Bergamin Filho A (2006) Effect of temperature and leaf wetness duration on infection of sweet oranges by Asiatic citrus canker. *Plant Pathology*, **55**, 657–663.

Darch G, Arkell B, Tradewell J (2011) *Water resource planning under climate uncertainty in London*. Atkins Report (Reference 5103993/73/DG/035) for the Adaptation Sub-Committee and Thames Water. Atkins, Epsom. Epsom.

DEFRA (2012) *UK climate change risk assessment. Government report*. The Stationery Office, London, UK.

Duthie JA (1997) Models of the response of foliar parasites to the combined effects of temperature and duration of wetness. *Phytopathology*, **87**, 1088–1095.

Fant C, Schlosser CA, Strzepek K (2015) The impact of climate change on wind and solar resources in southern Africa. *Applied Energy*, **161**, 556–564

Gamliel-Atinsky E, Sztejnberg A, Maymon M, Vintal H, Shtienberg D, Freeman S (2009) Infection dynamics of *Fusarium mangiferae*, causal agent of mango malformation disease. *Phytopathology*, **99**, 775–781.

Hay RKM, Russell G, Edwards TE (2000) *Crop Production in the East of Scotland*. Scottish Agricultural Science Agency, Edinburgh, UK.

Hueging H, Haas R, Born K, Jacob D, Pinto JG (2013) Regional changes in wind energy potential over Europe using regional climate model ensemble projections. *Journal of Applied Meteorology and Climatology*, **52**, 903–917.

Johnson DL, Erhardt RJ (2016) Projected impacts of climate change on wind energy density in the United States. *Renewable Energy*, **85**, 66–73.

de Jong MD, Bourdôt GW, Powell J, Goudriaan J (2002) A model of the escape of *Sclerotinia sclerotiorum* ascospores from pasture. *Ecological Modelling*, **150**, 83–105.

Kang Y, Khan S, Ma X (2009) Climate change impacts on crop yield, crop water productivity and food security – a review. *Progress in Natural Science*, **19**, 1665–1674.

Kerr A, Shackley S, Milne R, Allen S (1999) *Climate Change: Scottish Implications Scoping Study*. The Scottish Executive Central Research Unit, Edinburgh, UK.

van Keulen H, Stol W (1995) Agro-ecological zonation for potato production. In: *Potato Ecology and Modelling of Crops Under Conditions Limiting Growth* (eds Haverkort AJ, Mackerron DKL), pp. 357–371. Kluwer Academic Publishers, Dordrecht.

Kuparinen A, Katul G, Nathan R, Schurr FM (2009) Increases in air temperature can promote wind-driven dispersal and spread of plants. *Proceedings of the Royal Society of London B: Biological Sciences*, **276**, 3081–3087.

Launay M, Caubel J, Bourgeois G, Huard F, de Cortazar-Atauri IG, Bancal MO, Brisson N (2014) Climatic indicators for crop infection risk: application to climate change impacts on five major foliar fungal diseases in Northern France. *Agriculture, Ecosystems & Environment*, **197**, 147–158.

Liu B, Henderson M, Zhang Y, Xu M (2010) Spatiotemporal change in China's climatic growing season: 1955–2000. *Climatic Change*, **99**, 93–118.

Lobell DB, Gourdji SM (2012) The influence of climate change on global crop productivity. *Plant Physiology*, **160**, 1686–1697.

McKay MD, Beckman RJ, Conover WJ (1979) Comparison of three methods for selecting values of input variables in the analysis of output from a computer code. *Technometrics*, **21**, 239–245.

Monroe JS, Santini JB, Latin R (1997) A model defining the relationship between temperature and leaf wetness duration, and infection of watermelon by *Colletotrichum orbiculare*. *Plant Disease*, **81**, 739–742.

Overcamp TJ (1976) A general Gaussian diffusion-deposition model for elevated point sources. *Journal of Applied Meteorology*, **15**, 1167–1171.

Porter JR, Semenov MA (2005) Crop responses to climatic variation. *Philosophical Transactions of the Royal Society B: Biological Sciences*, **360**, 2021–2035.

Pryor SC, Barthelmie RJ (2010) Climate change impacts on wind energy: a review. *Renewable and Sustainable Energy Reviews*, **14**, 430–437.

Rötter R, van de Geijn SC (1999) Climate change effects on plant growth, crop yield and livestock. *Climatic Change*, **43**, 651–681.

Skelsey P (2008) *Multi-scale modeling of potato late blight epidemics*. PhD Thesis. Wageningen University, Wageningen.

Skelsey P, Newton AC (2014) Future environmental and geographic risks of Fusarium head blight of wheat in Scotland. *European Journal of Plant Pathology*, **142**, 133–147.

Skelsey P, Rossing WAH, Kessel GJT, Powell J, van der Werf W (2005) Influence of host diversity on development of epidemics: an evaluation and elaboration of mixture theory. *Phytopathology*, **95**, 328–338.

Skelsey P, van Der Werf W, Kessel GJT, Rossing WAH, Holtslag AAM (2007) Multiscale modelling of infection pressure from Phytophthora infestans. *EPPO Bulletin*, **37**, 313–316.

Skelsey P, Kessel GJT, Holtslag AAM, Moene AF, van der Werf W (2009a) Regional spore dispersal as a factor in disease risk warnings for potato late blight: a proof of concept. *Agricultural and Forest Meteorology*, **149**, 419–430.

Skelsey P, Kessel GJT, Rossing WAH, van der Werf W (2009b) Parameterization and evaluation of a spatiotemporal model of the potato late blight pathosystem. *Phytopathology*, **99**, 290–300.

Skelsey P, Rossing WAH, Kessel GJT, van der Werf W (2009c) Scenario approach for assessing the utility of dispersal information in decision support for aerially spread plant pathogens, applied to *Phytophthora infestans*. *Phytopathology*, **99**, 887–895.

Skelsey P, Rossing WAH, Kessel GJT, van der Werf W (2010) Invasion of *Phytophthora infestans* at the landscape level: how do spatial scale and weather modulate the consequences of spatial heterogeneity in host resistance? *Phytopathology*, **100**, 1146–1161.

Skelsey P, With K, Garrett K (2013) Why dispersal should be maximized at intermediate scales of heterogeneity. *Theoretical Ecology*, **6**, 203–211.

Sniffer (2014) Scotland's climate trends handbook. Available at: http://www.environment.scotland.gov.uk/climate_trends_handbook/index.html (accessed 15 January 2016).

Soares AR, Lourenço SA, Amorim L (2008) Infection of guava by *Colletotrichum gloeosporioides* and *Colletotrichum acutatum* under different temperatures and wetting periods. *Tropical Plant Pathology*, **33**, 265–272.

Sparks AH, Forbes GA, Hijmans RJ, Garrett KA (2014) Climate change may have limited effect on global risk of potato late blight. *Global Change Biology*, **20**, 3621–3631.

Spinoni J, Vogt J, Barbosa P (2015) European degree-day climatologies and trends for the period 1951–2011. *International Journal of Climatology*, **35**, 25–36.

Spitters CJT, van Keulen H, van Kraalingen DWG (1989) A simple and universal crop growth simulator: SUCROS87. In: *Simulation and Systems Management in Crop Protection* (eds Rabbinge R, Ward SA, Van Laar HH), pp. 147–181. Centre for Agricultural Publishing and Documentation, Wageningen, The Netherlands.

Stevenson WR (1993) Management of early blight and late blight. In: *Potato Health Management* (ed. Rowe RC), pp. 141–147. APS Press, St. Paul, MN.

Stewart HE, Taylor K, Wastie RL (1983) Resistance to late blight in foliage (*Phytophthora infestans*) of potatoes assessed as true seedlings and as adult plants in the glasshouse. *Potato Research*, **26**, 363–366.

Tobin I, Vautard R, Balog I *et al.* (2015) Assessing climate change impacts on European wind energy from ENSEMBLES high-resolution climate projections. *Climatic Change*, **128**, 99–112.

de Visscher A (2013) *Air Dispersion Modeling: Foundations and Applications*. John Wiley & Sons, Hoboken, NJ.

Zhang X, White RP, Demir E *et al.* (2014) *Leptosphaeria* spp., phoma stem canker and potential spread of *L. maculans* on oilseed rape crops in China. *Plant Pathology*, **63**, 598–612.

